Anti-Müllerian hormone and its receptor is colocalized in the majority of gonadotropin-releasing-hormone cell bodies and fibers in heifer brains

O. Kereilwe[a], **H. Kadokawa**[a*]

[a]*Faculty of Veterinary Medicine, Yamaguchi University, Yamaguchi-shi, Yamaguchi-ken 1677-1, Japan.*

*Corresponding author.

Tel.: + 81 83 9335825; fax: +81 83 9335938

E-mail address: hiroya@yamaguchi-u.ac.jp (H. Kadokawa)

ABSTRACT

Circulating concentrations of Anti-Müllerian hormone (AMH) can indicate fertility in various animals, but the physiological mechanisms underlying the effect of AMH on fertility remain unknown. We recently discovered that AMH has extragonadal functions via its main receptor, AMH receptor type 2 (AMHR2). Specifically, AMH stimulates the secretion of luteinizing hormone and follicle stimulating hormone from bovine gonadotrophs. Moreover, gonadotrophs themselves express AMH to exert paracrine/autocrine functions, and AMH can activate gonadotropin-releasing-hormone (GnRH) neurons in mice. This study aimed to evaluate whether AMH and AMHR2 are detected in areas of the brain relevant to neuroendocrine control of reproduction: the preoptic area (POA), arcuate nucleus (ARC), and median eminence (ME), and in particular within GnRH neurons. Reverse transcription-polymerase chain reaction detected both *AMH* and *AMHR2* mRNA in tissues containing POA as well as in those containing both ARC and ME, collected from post-pubertal heifers. Western blotting detected AMH and AMHR2 protein in the collected tissues. Triple fluorescence immunohistochemistry revealed that the majority of cell bodies or fibers of GnRH neurons were AMHR2-positive and AMH-positive, although some were negative. Immunohistochemistry revealed that 75 to 85% of cell bodies and fibers of GnRH neurons

were positive for both AMH and AMHR2 in the POA, ARC, and both the internal and external zones of ME. The cell bodies of GnRH neurons were situated around other AMH-positive cell bodies or fibers of GnRH and non-GNRH neurons. Our findings thus indicate that AMH and AMHR2 are detected in the majority of cell bodies or fibers of GnRH neurons in POA, ARC, or ME of heifer brains. These data support the need for further study as to how AMH and AMHR2 act within the hypothalamus to influence GnRH and gonadotropin secretion.

Keywords:

Anti-Mullerian hormone receptor type 2; Arcuate nucleus; Gonadotropin-releasing hormone neuron; Preoptic area; External zone of the median eminence; Ruminants

Highlights*:*

- AMH and AMHR2 are detected in the bovine POA, ARC, and ME, including the external zone of ME.
- Majority of cell bodies or fibers of GnRH neurons are positive for both AMH and AMHR2 in the POA, ARC, or ME.

There are also GnRH-negative AMHR2-positive cell bodies or fibers of neurons, and GnRH-negative AMH-positive cell bodies or fibers of neurons.

1. Introduction

The hypothalamic-pituitary-gonadal axis drives reproduction and some of the most important components of the axis are the gonadotropin-releasing-hormone (GnRH) neurons [1, 2]. GnRH neurons originate in the preoptic area (POA) and arcuate nucleus (ARC) and project to the median eminence (ME), the interface between the neural and peripheral endocrine systems, and secrete GnRH into the pituitary portal blood vessels [3, 4]. The secreted GnRH binds to the GnRH receptors on the lipid raft portion of the plasma membrane of gonadotrophs to stimulate the secretion of luteinizing hormone (LH) and follicle stimulating hormone (FSH) [5]. It is thus important to clarify mechanisms controlling GnRH neurons in the hypothalamus.

Anti-Mullerian hormone (AMH) is a glycoprotein that belongs to the transforming growth factor (TGF)-β superfamily, which includes inhibin and activin. The best-studied tissue that secretes AMH are the immature granulosa cells in the ovaries of adult humans and animals [6] and AMH reportedly plays various important roles therein [7, 8]. Interestingly, plasma AMH concentrations can predict the fertility of adult female goats, ewes, cows, and women [9-11]. Recent studies have revealed that AMH exerts extragonadal functions in the gonadotrophs of the anterior pituitaries. The main AMH receptor, AMH receptor type 2 (AMHR2), colocalizes with GnRH receptors on the lipid raft of gonadotrophs [12]. Furthermore, AMH activates AMHR2 and thereby stimulates

73 the synthesis and secretion of LH and FSH in the gonadotrophs of bovines and rodents
74 [12-14]. However, it remains unknown whether AMH and AMHR2 play any significant
75 roles in the hypothalamus.

76 Little is known concerning the relationship between AMH and the brain. While the
77 brains of adult tilapia express AMH, the localization of AMH expression in the brain
78 remains unclarified [15]. Another recent study found that GnRH neurons contain AMHR2
79 in various regions of female human and rodent brains, including the POA, ARC, and ME
80 [16]. Furthermore, both *in vivo* and *in vitro* studies have demonstrated that AMH potently
81 activates GnRH neurons, and consequently GnRH-dependent LH secretion in adult
82 female mice [16]. However, it remains unknown as to whether female mammalian brains
83 express AMH. Therefore, this study evaluated whether AMH and AMHR2 are detected
84 in the POA, ARC, and ME of heifers, and especially within GnRH neurons.

85

86 **2. Materials and Methods**

87 *2.1 Brain and ovary sample collection*

88 All experiments were performed in accordance with the Guiding Principles for the
89 Care and Use of Experimental Animals in the Field of Physiological Sciences
90 (Physiological Society of Japan) and were approved by the Committee on Animal

91 Experiments of Yamaguchi University.

92 We obtained brain samples from healthy, post-pubertal (26 months of age) non-
93 lactating Japanese Black heifers managed by our contracted farmers in western Japan.
94 The farms had open free stall barns with free access to water. The heifers were fed twice
95 daily with a total mixed ration according to the Japanese feeding standard [17].

96 The heifers were slaughtered for harvesting beef according to the regulation of
97 Ministry of Agriculture, Forestry and Fisheries of Japan. The heifers were in periestrus –
98 i.e., -3 d to +4 d from estrus – as determined by macroscopic examination of the ovaries
99 and uterus [18]. We used the samples (n = 5) obtained from the periestrus period for the
100 following three reasons. First, there is no difference in GnRH immunoreactivity in the
101 bovine POA, ARC, and ME between the periestrus and diestrus phases, however, while
102 kisspeptin immunoreactivity in the bovine POA and ME does not differ between the
103 periestrus and diestrus phases, it is higher in the periestrus phase than in the diestrus phase
104 in the ARC [19]. Second, the promoter regions of bovine AMH and AMHR2 genes lack
105 the consensus response element for estrogen and progesterone [12, 20]. Third, there are
106 no changes in AMH and AMHR2 expression in the anterior pituitary gland [12, 20] or in
107 blood AMH concentrations during the estrous cycle [21]. We followed a method
108 established by previous studies to collect brain block samples from cows to perform

109 immunohistochemistry [19]. Briefly, blocks were dissected with the following margins:
110 rostrally-rostral border of the optic chiasm; caudally-rostral to the mammillary bodies;
111 lateral to the optic chiasm; and 0.5 cm dorsal to the third ventricle. We then followed
112 previously reported methods [22] for splitting the block into two parts by cutting rostral
113 to the ME, yielding an anterior part containing the POA (POA block) and a posterior part
114 containing the ARC and ME (ARC&ME block). Each block was stored in 4%
115 paraformaldehyde at 4° C for 24 h. The fixed blocks were placed in a 20% sucrose
116 solution at 4° C for 72 h. They were then stored in 30% sucrose solution at 4° C until the
117 block sank – at least 48 h. Serial coronal sections were cut into 50 µm thick sections using
118 a cryostat (CM1900, Leica Microsystems Pty Ltd., Wetzlar, Germany).

119 We used previous papers showing an atlas of bovine brain sections as a guide [23, 24].
120 Briefly, sections were cut while monitoring (from both anterior and lateral views) the
121 shape of the third ventricle and ventral or dorsal edge line, and the position and size of
122 the anterior commissure, optic chiasm, mammilothalamic tract, or fornix. The selected
123 POA tissues contained both anterior commissure or optic chiasm, and POA was medial
124 or lateral to the third ventricle, similar to Fig 8, 9 , and 10 in Okamura [23] and Fig 2E
125 and 2F in Leshin *et al.* [24].The selected ARC&ME tissues contained fornix and ARC
126 adjacent to both the evident infundibular recess of third ventricle and the median

eminence which attached to infundibulum, the same as Fig. 18, 19, and 20 of the atlas [23] and Fig2E, F of another atlas [24]. Every sixth section of the tissue was subjected to triple immunostaining for GnRH, AMH, and AMHR2. At least four sections from the rostral end of the organum vasculosum of the lamina terminalis to the rostral edge of the hypothalamic paraventricular nucleus were used for the POA. At least four sections from the rostral edge of the dorsomedial hypothalamic nucleus to the rostral edge of the mammillary bodies were used for the ME and ARC. As performed in a previous study [22], the sections were then stored in 25 mM PBS containing 50% glycerol, 250 mM sucrose, and 3.2 mM $MgCl_2 \cdot 6H_2O$ at -20°C until used for immunohistochemistry.

We also collected POA and ARC&ME tissue samples from other periestrous heifers (n = 5) to perform reverse transcription-polymerase chain reaction (RT-PCR) or western blotting. Both POA and ARC&ME blocks were cut at their midlines to obtain left and right sides. Using the bovine brain atlas [23, 24] as a reference, the blocks were further cut using their exterior shapes and the third or lateral ventricles as landmarks. Finally, the size of each tissue sample containing POA was less than 1 cm along its lateral axis; 2 cm along the rostrocaudal axis; and 3 cm along the vertical axis. The size of each tissue containing the ARC&ME was less than 1 cm along its lateral axis; 2 cm along the rostrocaudal axis; and 1 cm along the vertical axis. The POA and ARC&ME tissues were

145 immediately frozen in liquid nitrogen and stored at −80° C until RNA or protein extraction.

146 Granulosa cells in preantral and small antral follicles express AMH [25] and AMHR2

147 mRNA [26]. Therefore, we also collected ovary tissue samples from the same heifers to

148 use as a positive-controls for AMH and AMHR2 in the RT-PCR (n = 5) and western

149 blotting (n = 5) analyses.

150

151 *2.2 RT-PCR, sequencing of amplified products, and homology search in gene databases*

152 We used previously reported RT-PCR and sequencing methods [12, 20] in order to

153 detect AMH or AMHR2 mRNA in the POA tissue (n = 5) and ARC&ME tissue (n = 5).

154 Briefly, total RNA was extracted from the either side of POA or ARC & ME tissue as

155 well as the ovary samples (used as positive controls) using mortar, liquid nitrogen, and

156 RNAzol RT Reagent (Molecular Research Center Inc., Cincinnati, OH, USA) according

157 to the manufacturer's protocol. The extracted RNA samples were treated with

158 ribonuclease-free deoxyribonuclease (Thermo Fisher Scientific, Waltham, MA, USA) to

159 eliminate possible genomic DNA contamination. The concentration and purity of each

160 RNA sample were evaluated to ensure the A_{260}/A_{280} nm ratio measured by

161 spectrophotometer was in the acceptable range of 1.8 to 2.1. The mRNA quality of all

162 samples was verified by electrophoresis of total RNA followed by staining with ethidium

bromide, and the 28S:18S ratios were 2:1. Complementary DNA was synthesized from 2 μg of the total RNA per sample using Verso cDNA synthesis Kit (Thermo Fisher Scientific). PCRs were conducted using the previously reported primers (Table 1) [12, 20], which were designed by Primer3 based on reference sequence of bovine AMH [National Center for Biotechnology Information (NCBI) reference sequence of bovine AMH is NM_173890] or bovine AMHR2 (NCBI reference sequence is NM_001205328.1). The expected PCR-product sizes of AMH and AMHR2 using the primer pairs are 328 bp, and 320 bp, respectively. PCR was performed using 20 ng of cDNA and polymerase (Tks Gflex DNA Polymerase, Takara Bio Inc., Shiga, Japan) under the following thermocycles: 94°C for 1 min for pre-denaturing followed by 35 cycles of 94°C for 60 s, 60°C for 15 s, and 68°C for 30 s. PCR products were separated on a 1.5% agarose gel by electrophoresis with a molecular marker [Gene Ladder 100 (0.1 to 2 kbp), Nippon Gene, Tokyo, Japan], stained with fluorescent stain (Gelstar, Lonza, Allendale, NJ), and observed using a charge-coupled device (CCD) imaging system (GelDoc; Bio-Rad, Hercules, CA, USA). The PCR products were purified with the NucleoSpin Extract II kit (Takara Bio Inc.) and then sequenced with a sequencer (ABI3130, Thermo Fisher Scientific) using one of the PCR primers and the Dye Terminator v3.1 Cycle Sequencing Kit (Thermo Fisher Scientific). The sequences

obtained were used as query terms with which to search the homology sequences in the DNA Data Bank of Japan/GenBank/European Bioinformatics Institute Data Bank using the basic nucleotide local alignment search tool (BLAST) optimized for highly similar sequences (available on the NCBI website).

2.3 Antibodies used in this study

We used anti-human AMH and anti-bovine AMHR2 antibodies, whose efficacies were previously verified with bovine ovaries and anterior pituitaries [12, 20], to detect AMH and AMHR2 proteins in bovine brain samples via western blotting and immunohistochemistry. The anti-human AMH rabbit polyclonal antibody (ARP54312_P050; Aviva Systems Biology, CA, USA) recognizes the mature C-terminal form of human AMH (corresponding to amino acids 468 to 517; SVDLRAERSVLIPETYQANNCQGVCGWPQSDRNPRYGNHVVLLLKMQARG) [20]. This sequence had 98% homology to amino acids 483 to 532 of the mature C-terminal form of bovine AMH but no homology to other bovine proteins, as determined using protein BLAST. Our original anti-bovine AMHR2 chicken polyclonal antibody recognizes the extracellular region that is located near the N-terminus of the bovine AMHR2 (corresponding to amino acids 31 to 45; GVRGSTQNLGKLLDA) [12].

We also used an anti-GnRH mouse monoclonal antibody (clone number GnRH I HU11B: sc-32292, Santa Cruz Biotechnology, Inc., Dallas, TX, USA) raised against a synthetic GnRH I decapeptide by Urbanski (1991) [27]. This antibody was used for immunohistochemistry to visualize GnRH neurons in rat and monkey [28, 29].

2.4 Western Blotting for AMH or AMHR2 detection

The western blotting in our previous studies [12, 20] showed similar bands of AMHR2 and AMH in the anterior pituitaries and ovaries; however, there are a few differences in the band size between the two tissues, probably because of the differences in glycosylation [30-32]. Therefore, we used a previously reported method of western blotting to detect AMH or AMHR2 [12, 20]. Briefly, proteins were extracted from the frozen-stock POA (n = 5), ARC & ME (n = 5), or ovary samples (n = 5, used as positive controls) utilizing mortar, liquid nitrogen, and a tissue protein extraction reagent (T-PER; Thermo Fisher Scientific) with protease inhibitors (Halt Protease Inhibitor Cocktail; Thermo Fisher Scientific). The total protein content of each tissue homogenate was estimated using the bicinchoninic acid kit (Thermo Fisher Scientific). The extracted protein sample (33.4 µg of total protein in 37.5 µL) was mixed in 12.5 µL of 4x Laemmli sample buffer (Bio-rad) containing 10% (v/v) β-mercaptoethanol, then boiled for 3 min

217 at 100 °C. The boiled protein samples were quickly cooled down in ice. The protein
218 samples (8 µg of total protein) were loaded onto a polyacrylamide gel along with a
219 molecular weight marker (Precision Plus Protein All Blue Standards; Bio-Rad), and
220 resolved by electrophoresis on sodium dodecyl sulfate polyacrylamide gels at 100 V for
221 90 min. Proteins were then transferred to polyvinylidene fluoride (PVDF) membranes.
222 Blocking was done with 0.1% Tween 20 and 5% non-fat dry milk for 1 h at 25 °C then
223 immunoblotting was performed with the anti-AMH rabbit antibody or anti-AMHR2
224 chicken antibody (1:25,000 dilution each) overnight at 4 °C. After washing the
225 membrane with 10 mM Tris–HCl (pH 7.6) containing 150 mM NaCl and 0.1% Tween
226 20, the PVDF membrane was incubated with horseradish peroxidase (HRP)-conjugated
227 goat antibody against rabbit IgG or anti-chicken IgG (Bethyl laboratories, Inc.,
228 Montgomery, TX, USA; 1:50,000 dilution) at 25 °C for 1 h. Protein bands were
229 visualized using an ECL-Prime chemiluminescence kit (GE Healthcare, Amersham,
230 UK) and a CCD imaging system (Fujifilm, Tokyo, Japan). In accordance with previous
231 studies [33-35], we defined bovine AMH bands based on their mobility as the AMH
232 precursor or the mature form (four sizes). Further, we defined bovine AMHR2 bands
233 based on their mobility as dimers, full-length monomers, or cleaved monomers,
234 according to previously reported methods [30, 36]. Antibodies were removed from the

PVDF membrane with stripping solution (Nacalai Tesque Inc., Kyoto, Japan) prior to immunoblotting with an anti-β-actin mouse monoclonal antibody (A2228, 1:50,000 dilution; Sigma-Aldrich, St. Louis, MO, USA).

2.5 Fluorescent immunohistochemistry and confocal microscopy

The frozen-stock POA or ARC&ME tissue was thawed and washed twice with PBS. Free-floating tissue sections were permeabilized with PBS containing 0.5% Tween 20 for 3 min. We then combined two quenching methods, glycine/hydrogen peroxide [37] and Vector True VIEW autofluorescence quenching kit (Vector Laboratories Inc., Burlingame, CA, USA), because we observed tissue autofluorescence in a preliminary study. Briefly, the tissue was blocked with PBS containing 2% normal goat serum, 50 mM glycine, 0.05% Tween 20, 0.1% Triton X 100, and 0.1% BSA for 30 min [37]. We subsequently employed Vector True VIEW autofluorescence quenching kit following the manufacturer's protocol. After 5 min of incubation with the quencher kit, the sections were washed twice with PBS. The sections were then incubated with a cocktail of primary antibodies (anti-GnRH mouse, anti-AMH rabbit, and anti-AMHR2 chicken antibodies [all diluted as 1:1,000]) dissolved in PBS containing 10 mM glycine, 0.05% Tween 20, 0.1% Triton X 100, and 0.1% hydrogen peroxide at 4° C for 16 h. After the primary

253 antibody incubation, the sections were washed twice with PBS and then incubated with a
254 cocktail of fluorochrome-conjugated secondary antibodies (Alexa Fluor Alexa Fluor 488
255 goat anti-chicken IgG, Alexa Fluor 546 goat anti-mouse IgG, and Alexa Fluor 647 goat
256 anti-rabbit IgG [all from Thermo Fisher Scientific and diluted to 1 µg/mL]) and 1 µg/mL
257 of 4′, 6′-diamino-2-phenylindole (DAPI; Wako Pure Chemicals, Osaka, Japan) for 4 h at
258 room temperature. Each free-floating section was then transferred onto a slide glass (76
259 × 26 mm, Crest-adhesive glass slide, Matsunami-Glass, Osaka, Japan) with the dorsal-
260 ventral axis of the bovine brain section parallel to the long axis of slides. Cover glass (55
261 × 24 mm, Neo micro cover glass, Matsunami-Glass) was then attached using Vectashield
262 hardset mounting medium (Vector Laboratories Inc.).

263 The sections were observed with a confocal microscope (LSM710; Carl Zeiss,
264 Göttingen, Germany) equipped with a 405 nm diode laser, a 488 nm argon laser, a 533
265 nm HeNe laser, and a 633 nm HeNe laser. Images obtained by fluorescence microscopy
266 were scanned with a 20× or 40× oil-immersion objective and recorded with a CCD camera
267 system controlled by ZEN2012 black edition software (Carl Zeiss). GnRH, AMH, and
268 AMHR2 localization were examined in confocal images of triple-immunolabeled
269 specimens. To verify the specificity of the signals, we included several negative controls
270 in which the primary antiserum had been omitted or pre-absorbed with 5 nM of the

antigen peptide [12, 20], or in which normal rabbit IgG (Wako Pure Chemicals) was used instead of the primary antibody.

We distinguished the internal zone (iME; ventral to third ventricle) and the external zone on the ME (eME) based on differences in fluorescence intensity. We defined various segments of neurons based on the following criteria: cell body is round or polygonal shape and diameter is more than 8 μm; axon is shown as a continuous line of immunopositive signal; varicosity is shown as a dotted line; bouton is shown as a single dot with a diameter more than 3μm. In the POA, ARC, and iME, we decided on the presence of a fiber of neuron if the axon, or varicosity were observed in these areas; whereas we decided on the presence of a fiber of neuron if axon, varicosity, or bouton were observed in the eME. We specified GnRH neuron if the neuron had a similar shape compared to the previous paper reporting bovine GnRH neuron [24] and showed GnRH-positive signal (red color).

To evaluate colocalization, the GnRH signal was shown in red and either AMH or AMHR2 was shown in green. Therefore, yellow coloration in the images indicated colocalization of GnRH with AMH or AMHR2. The percentage of cell bodies or fibers of GnRH single-labeled neurons and the percentage of double/triple-labeled cell bodies or fibers of neurons among all of the GnRH-positive cell bodies or fibers of neurons were determined in the POA, ARC, iME, or eME of five heifers. From each heifer, four sections

289 containing the POA and four sections containing the anterior or intermediate part of the
290 ARC, iME, and eME with a similar shape to those shown in Fig. 18 and 19 of the atlas
291 [23] were analyzed.

292 Additionally, z-stacks of the optical sections of triple-labeled cell bodies in POA
293 tissues or triple-labeled fibers in eME were captured using a confocal microscope system
294 and transparent projection (i.e., the strongest and nearest colors to observer were shown).
295 Images of the confocal microscope findings were generated using ZEN2012 black edition
296 software (Carl Zeiss). To evaluate colocalization, the signals corresponding to AMHR2,
297 GnRH, and AMH are depicted in green, red, and blue, respectively.

298

299 **3. Results**

300 *3.1 Detection of AMH* and *AMHR2 mRNA in POA and ARC&ME tissues*

301 The agarose gel electrophoresis yielded PCR products of the expected sizes,
302 indicating that AMH (328 bp; Fig. 1A) and AMHR2 (320 bp; Fig. 1B) were amplified
303 from the POA and ARC&ME tissues. The same was found for the PCR products obtained
304 from ovary tissues. Homology searching for the obtained sequences of amplified products
305 in the gene databases revealed that the best match alignment was bovine *AMH*
306 (NM_173890.1) or bovine *AMHR2* (NM_001205328.1). Both had a query coverage of

100%, an e-value of 0.0, and a maximum alignment identity of 99%. No other bovine gene was found to have homology with the obtained sequences of the amplified products, thus showing that the sequences of the amplified products were identical with the sequences of bovine AMH or AMHR2.

3.2 Detection of AMH and *AMHR2 protein in POA and ARC&ME tissues*

Western blotting confirmed the presence of AMH in the POA, ARC&ME, and ovary tissues, with differences in intensity among sample types (Fig. 2A). Unlike in the ovary samples, no bands for the AMH precursor (70 kDa) were detected in the POA or ARC&ME samples. Stronger bands for the mature C-terminal form were observed in the POA and ARC&ME samples than in the ovary samples, and differences in the number of bands were found between those of POA, ARC&ME (25 kDa and 20 kDa), and ovary (25 kDa only) samples. Figure 2A' shows representative β-actin bands for each sample.

Western blotting confirmed the presence of AMHR2 in POA, ARC&ME, and ovary tissues (Fig. 2B). While the anti-AMHR2 antibody revealed similar bands in the three tissues, a few differences were noted. The full-length and cleaved monomers in the ovary appeared as a single band but appeared as a doublet in the POA. Figure 2B' shows representative β-actin bands for both tissue types.

325

326 *3.3 Immunofluorescence analysis of AMH and AMHR2*

327 The triple fluorescence immunohistochemistry detected AMH, AMHR2, and GnRH
328 in the POA and ARC&ME tissues. Figure 3 diagrammatically presents the distribution of
329 GnRH-positive, AMH-positive or AMHR2-positive cell bodies and fibers. This drawn
330 distribution represents a pattern typical to all heifers studied. The triple-positive (GnRH-
331 positive, AMH-positive and AMHR2-positive) cell bodies and fibers (green in Fig. 3)
332 were observed in distribution extending from the preoptic region to the hypothalamic area.
333 GnRH neurons were shown as cell bodies with varicosities, or axons (CB1 and CB2 in
334 Fig.4). The clusters of 2-10 cells were observed (Fig. 4, 6).

335 In the preoptic region, the triple positive cell bodies were abundant in the anterior
336 medial preoptic area (MPOA) and anterior preoptic area (Fig. 3A, 3B), but were less
337 frequently observed in the posterior MPOA and POA (Fig. 3C). We observed that the
338 majority of cell bodies and fibers of GnRH neurons were AMHR2-positive and AMH-
339 positive (CB1, CB3-8, and CB10,11 in Fig.4). Figure 5 presents a transparent projection
340 of the z-stack images of triple-stained cell bodies and fibers in the POA, with AMHR2,
341 GnRH, and AMH depicted in green, red, and blue, respectively. The three colors were
342 mixed in almost all areas. However, we also observed AMHR2-negative, AMH-negative

343 cell bodies or fibers of GnRH neurons (CB2) , as less frequently in the anterior MPOA
344 and POA (red cross in Fig. 3A). We also less frequently observed GnRH-negative
345 AMHR2 cell bodies (CB9). The AMHR2-positive and AMH-positive cell bodies of
346 GnRH neurons were observed in close proximity (within 5 μm) to cell bodies of another
347 GnRH neuron, as shown in CB2 and CB3, CB6 and CB7, and CB10 and CB11.

348 In the anterior ARC, we observed that all of the GnRH cell bodies were AMHR2-
349 positive and AMH-positive (CB1-5 in Fig. 6), although the triple positive cell bodies were
350 only occasionally observed (Fig. 3D, 3E), and not in the posterior ARC (Fig. 3F). We
351 observed that majority of GnRH fibers were AMHR2-positive and AMH-positive (Fig.
352 6**A**, 6**C**, 6**D**), although we also observed AMHR2-positive AMH-negative GnRH fibers
353 (Fig.**5**B). The triple-positive cell bodies or fibers of neurons were observed in close
354 proximity (within 5 μm) as shown in CB1 and CB2, and CB4 and CB5.

355 In the iME, we observed that the majority of fibers of GnRH neurons were AMHR2-
356 positive and AMH-positive (low magnification of Fig. 7A, B, and Fig. 8A, yellow Vs in
357 Enlarged 1, 2, 3), although we also observed AMHR2-negative, AMH-negative
358 varicosities of GnRH neurons (red Vs in Enlarged 2, 3). These fibers were observed in
359 close proximity (within 5 μm), as shown (Enlarged 2, 3).

In the eME, we observed that the majority of fibers of GnRH neurons were AMHR2-positive and AMH-positive (yellow arrows in Enlarged 1 and 2 in Fig. 8); we also observed AMHR2-negative, AMH-negative fibers of GnRH neurons (red arrows in Enlarged 2), and GnRH-negative fibers of AMH neurons (blue arrows in Enlarged 2). Figure 9 presents a transparent projection of the z-stack images of triple-stained fibers (Fig. 9A) and the terminal (Fig. 9B) in eME. AMHR2, GnRH, and AMH signals are depicted in green, red, and blue, respectively. These colors were mixed in almost all parts of the fibers, whereas, most areas of the terminal exhibited only GnRH and AMH staining.

Table 2 and Table 4 show the number of examined GnRH-positive, AMHR2-positive, or AMH-positive cell bodies and fibers in the POA, ARC, iME, or eME. As shown in Table 3 and Table 5, 75 to 85% of cell bodies and fibers of GnRH neurons are positive for both AMH and AMHR2 in the POA, ARC, and both the internal and external zones of ME.

4. Discussion

The present study detected AMH and AMHR2 in the bovine POA, ARC, and ME. To the best of our knowledge, this study is the first to report AMH in the brains of mammals and AMHR2 in the brains of ruminants. The discovered AMH and AMHR2 in

the POA, ARC, and ME warrant further exploration because their localization have significant implications for reproduction.

In the POA, ARC and ME, we observed that the majority of cell bodies or fibers of GnRH neurons were AMHR2-positive and AMH-positive. Little is known of the relationship between AMH and GnRH neurons. However, Cimino *et al.* [16] reported that (1) more than 50% of mouse and human GnRH neurons express AMHR2, and (2) AMH directly activates 50 to 64% of GnRH neurons in a dose-dependent manner in mice. The great majority of GnRH neurons (86%) form multiple close appositions with dendrites of other GnRH neurons, probably for GnRH neuron synchronization via the dendro-dendritic communication [38]. Therefore, AMH and AMHR2 in GnRH neurons might indeed be relevant to the regulation of GnRH secretion by direct actions on GnRH neurons. Further studies are required to clarify the importance of AMH and AMHR2 in the regulation of GnRH neurons.

GnRH neurons in the POA and ARC project to the ME and secrete GnRH into the pituitary portal blood vessels [3, 4]. Cimino *et al.* [16] observed AMHR2 in the eME in mice and women. In addition, the present study found AMH signals in the bovine eME. Intracerebroventricular injection of AMH induces a LH surge within 15 min in mice [16]. AMHR2 is expressed in bovine gonadotrophs, and AMH can stimulate LH and FSH

396 secretion from the cultured bovine gonadotrophs [12]. Therefore, AMH may be secreted
397 into the pituitary portal blood to stimulate LH and FSH secretion from gonadotrophs.
398 There is one caveat to our study that should be considered: both the POA and
399 ARC&ME specimens also contained other brain areas and nuclei because it was
400 impossible to obtain precisely cut samples under our experimental conditions. However,
401 western blotting conducted in the present study showed differences in band strength
402 and/or size between brains and ovaries. Unlike findings obtained from ovary samples, the
403 POA and ARC&ME exhibited no bands that indicated the presence of the AMH precursor
404 (70 kDa), suggesting that cells in POA and ARC&ME store fewer AMH precursors than
405 do ovaries. Two bands for the mature C-terminal form were observed in the POA and
406 ARC&ME, whereas only a single band was observed in the ovary (25 kDa). The band-
407 size variances in the mature C-terminal band may be ascribed to differences in O-
408 glycosylation among organs [31, 32]. Western blotting also revealed multiple, not single,
409 bands of AMHR2, which has been reported previously. This may be explained by
410 AMHR2 presenting as a dimer, full-length monomer, and cleaved monomers, and by
411 AMHR2 having O-glycosylation [30, 35]. We observed that full-length and cleaved
412 monomers in the POA appeared as doublets, whereas those in the ovary appeared as single
413 bands. Therefore, this study suggests that bovine AMHR2 is glycosylated and that the

414 difference in the number of full-length monomers between the POA and ovary samples
415 might be attributed to differences in glycosylation.

416 AMHR2 positive non-GnRH cells were observed in the POA, ARC, and ME. We
417 could not find any related published data with which to compare our findings. Therefore,
418 further studies are required to characterize this type of neuron, specifically, whether
419 AMHR2 is expressed in kisspeptin, neurokinin B, dynorphin neurons of the ARC [2].
420 AMH signals were observed in non-GnRH cells in the eME. The localization of AMH in
421 the eME has not been previously examined in any species to our knowledge.
422 Approximately 20% of AMHR2-positive cells are non-gonadotrophs in the bovine
423 anterior pituitary [12], and such cells may be lactotrophs [39]. Further studies are required
424 to evaluate the relationship between AMH in the sME and non-gonadotroph anterior
425 pituitary cells.

426 In conclusion, AMH and AMHR2 are detected in the majority of GnRH neurons
427 in POA, ARC, and ME of heifer brains. These data support the need for further study as
428 to how AMH and AMHR2 act within the hypothalamus to influence GnRH and
429 gonadotropin secretion.

430

431 **Credit authorship contribution statement**

O. Kereilwe: Conceptualization, Methodology, Formal analysis, Investigation, Writing - original draft, Visualization.

H. Kadokawa: Conceptualization, Supervision, Methodology, Formal analysis, Investigation, Writing - original draft, Funding acquisition.

Acknowledgements

O. Kereilwe was supported by MEXT (Ministry of Education, Culture, Sports, Science, and Technology) with the provision of a scholarship.

This research was partly supported by a Grant-in Aid for Scientific Research (JSPS Kakenhi Grant Number 18H02329) from the Japan Society for the Promotion of Science (Tokyo, Japan) to H. Kadokawa.

Conflicts of interest: The authors declare no conflicts of interest.

Ethical considerations: The study was approved by the Committee on Animal Experiments of Yamaguchi University, and complied with relevant legislation.

References

[1] Herbison AE. Control of puberty onset and fertility by gonadotropin-releasing hormone neurons. Nat Rev Endocrinol 2016;12:452-66.

[2] Nestor CC, Bedenbaugh MN, Hileman SM, Coolen LM, Lehman MN, Goodman RL. Regulation of GnRH pulsatility in ewes. Reproduction 2018;156:R83-R99.

[3] Clarke IJ, Cummins JT, Karsch FJ, Seeburg PH, Nikolics K. GnRH-associated peptide (GAP) is cosecreted with GnRH into the hypophyseal portal blood of ovariectomized sheep. Biochem Biophys Res Commun 1987;143:665-71.

[4] Jansen HT, Hileman SM, Lubbers LS, Kuehl DE, Jackson GL, Lehman MN. Identification and distribution of neuroendocrine gonadotropin-releasing hormone neurons in the ewe. Biol Reprod 1997;56:655-62.

[5] Kadokawa H, Pandey K, Nahar A, Nakamura U, Rudolf FO. Gonadotropin-releasing hormone (GnRH) receptors of cattle aggregate on the surface of gonadotrophs and are increased by elevated GnRH concentrations. Anim Reprod Sci 2014;150:84-95.

[6] Bhide P, Homburg R. Anti-Müllerian hormone and polycystic ovary syndrome. Best Pract Res Clin Obstet Gynaecol 2016;37:38-45.

[7] Hernandez-Medrano JH, Campbell BK, Webb R. Nutritional influences on folliculogenesis. Reprod Domest Anim Suppl 2012;4:274-82.

[8] Seifer DB, Merhi Z. Is AMH a regulator of follicular atresia? Assist Reprod Genet 2014;31:1403-07.

[9] Monniaux D, Drouilhet L, Rico C, Estienne A, Jarrier P, Touzé JL, Sapa J, Phocas F, Dupont J, Dalbiès-Tran R, Fabre S. Regulation of anti-Müllerian hormone production in domestic animals. Reprod Fertil Dev 2012;25:1-16.

[10] Meczekalski B, Czyzyk A, Kunicki M, Podfigurna-Stopa A, Plociennik L, Jakiel G, Maciejewska-Jeske M, Lukaszuk K. Fertility in women of late reproductive age: the role of serum anti-Müllerian hormone (AMH) levels in its assessment. J Endocrinol Invest 2016;39:1259-65.

[11] Mossa F, Jimenez-Krassel F, Scheetz D, Weber-Nielsen M, Evans ACO, Ireland JJ. Anti-Müllerian Hormone (AMH) and fertility management in agricultural species. Reproduction 2017;154:R1-R11.

[12] Kereilwe O, Pandey K, Borromeo V, Kadokawa H. Anti-Müllerian hormone receptor type 2 is expressed in gonadotrophs of postpubertal heifers to control gonadotrophin secretion. Reprod Fertil Dev 2018;30:1192-203.

[13] Bédécarrats GY, O'Neill FH, Norwitz ER, Kaiser UB, Teixeira J. Regulation of gonadotropin gene expression by Müllerian inhibiting substance. Proc Natl Acad Sci USA 2003;100:9348-53.

485 [14] Garrel G, Racine C, L'Hôte D, Denoyelle C, Guigon CJ, di Clemente, N., and Cohen-
486 Tannoudji, J. Anti-Müllerian hormone: a new actor of sexual dimorphism in pituitary
487 gonadotrope activity before puberty. Sci Rep 2016;6:23790.
488 [15] Poonlaphdecha S, Pepey E, Huang SH, Canonne M, Soler L, Mortaji S, Morand S,
489 Pfennig F, Mélard C, Baroiller JF, D'Cotta H. Elevated amh gene expression in the
490 brain of male tilapia (Oreochromis niloticus) during testis differentiation. Sex Dev
491 2011;5:33-47.
492 [16] Cimino I, Casoni F, Liu X, Messina A, Parkash J, Jamin SP, Catteau-Jonard S,
493 Collier F, Baroncini M, Dewailly D, Pigny P, Prescott M, Campbell R, Herbison AE,
494 Prevot V, Giacobini P. Novel role for anti-Müllerian hormone in the regulation of
495 GnRH neuron excitability and hormone secretion. Nat Commun 2016;7:10055.
496 [17] Agriculture, Forestry and Fisheries Research Council Secretariat. Nutrition
497 requirement. In: Ministry of Agriculture, Forestry and Fisheries, eds. Japanese
498 Feeding Standard for Beef Cattle. Tokyo, Japan: Central Association of Livestock
499 Industry; 2008:31–48.
500 [18] Miyamoto Y, Skarzynski DJ, Okuda K. Is tumor necrosis factor alpha a trigger for
501 the initiation of endometrial prostaglandin F(2alpha) release at luteolysis in cattle?
502 Biol Reprod 2000;62:1109-15.

503 [19] Tanco VM, Whitlock BK, Jones MA, Wilborn RR, Brandebourg TD, Foradori CD.
504 Distribution and regulation of gonadotropin-releasing hormone, kisspeptin, RF-
505 amide related peptide-3, and dynorphin in the bovine hypothalamus. PeerJ
506 2016;4:e1833.
507 [20] Kereilwe O, Kadokawa H. Bovine gonadotrophs express anti-Müllerian hormone
508 (AMH): comparison of AMH mRNA and protein expression levels between old
509 Holsteins and young and old Japanese Black females. Reprod Fertil Dev
510 2019;31:810-9.
511 [21] Koizumi M, Kadokawa H. Positive correlations of age and parity with plasma anti-
512 Müllerian hormone concentrations in Japanese Black cows. J Reprod Dev
513 2017;63:205-9.
514 [22] Hassaneen A, Naniwa Y, Suetomi Y, Matsuyama S, Kimura K, Ieda N, Inoue N,
515 Uenoyama Y, Tsukamura H, Maeda KI, Matsuda F, Ohkura S.
516 Immunohistochemical characterization of the arcuate kisspeptin/neurokinin
517 B/dynorphin (KNDy) and preoptic kisspeptin neuronal populations in the
518 hypothalamus during the estrous cycle in heifers. J Reprod Dev 2016;62:471-7.
519 [23] Okamura H. Brain atlas of cattle (in Japanese) In: A foundational research for
520 elucidation and estimation of agriculture, Forestry and Fisheries Research Council.

521 2002:41-72.
522 [24] Leshin LS, Rund LA, Crim JW, Kiser TE. Immunocytochemical localization of
523 luteinizing hormone-releasing hormone and proopiomelanocortin neurons within
524 the preoptic area and hypothalamus of the bovine brain. Biol Reprod 1988;39:963-
525 75.
526 [25] Campbell BK, Clinton M, Webb R. The role of anti-Müllerian hormone (AMH)
527 during follicle development in a monovulatory species (sheep). Endocrinology
528 2012;153:4533-43.
529 [26] Poole DH, Ocón-Grove OM, Johnson AL. Anti-Müllerian hormone (AMH) receptor
530 type II expression and AMH activity in bovine granulosa cells. Theriogenology
531 2016;86:1353-60.
532 [27] Urbanski HF. Monoclonal antibodies to luteinizing hormone-releasing hormone:
533 production, characterization, and immunocytochemical application. Biol Reprod
534 1991;44:681-6.
535 [28] Naugle MM, Gore AC. GnRH neurons of young and aged female rhesus monkeys
536 co-express GPER but are unaffected by long-term hormone replacement.
537 Neuroendocrinology 2014;100:334-46.
538 [29] Naugle MM, Lozano SA, Guarraci FA, Lindsey LF, Kim JE, Morrison JH, Janssen

539 WG, Yin W, Gore AC. Age and Long-Term Hormone Treatment Effects on the
540 Ultrastructural Morphology of the Median Eminence of Female Rhesus Macaques.
541 Neuroendocrinology 2016;103:650-64.
542 [30] Faure E, Gouédard L, Imbeaud S, Cate R, Picard JY, Josso N, di Clemente N. Mutant
543 isoforms of the anti-Müllerian hormone type II receptor are not expressed at the cell
544 membrane. J Biol Chem 1996;271:30571-5.
545 [31] Medzihradszky KF, Kaasik K, Chalkley RJ. Tissue-specific glycosylation at the
546 glycopeptide level. Mol Cell Proteomics 2015;14:2103-10.
547 [32] Skaar KS, Nobrega RH, Magaraki A, Olsen LC, Schulz RW, Male R. Proteolytically
548 activated, recombinant anti Mullerian hormone inhibits androgen secretion,
549 proliferation, and differentiation of spermatogonia in adult zebrafish testis organ
550 cultures. Endocrinology 2011;152:3527-40.
551 [33] Pierre A, Racine C, Rey RA, Fanchin R, Taieb J, Cohen-Tannoudji J, Carmillo P,
552 Pepinsky RB, Cate RL, di Clemente N. Most cleaved anti-Müllerian hormone binds
553 its receptor in human follicular fluid but little is competent in serum. J Clin
554 Endocrinol Metab 2016;101:4618-27.
555 [34] Mamsen LS, Petersen TS, Jeppesen JV, Møllgard K, Grøndahl ML, Larsen A, Ernst
556 E, Oxvig C, Kumar A, Kalra B, Andersen CY. Proteolytic processing of anti-

557 Mullerian hormone differs between human fetal testes and adult ovaries. Mol Hum
558 Reprod 2015;21:571–82.
559 [35] Di Clemente N, Jamin SP, Lugovskoy A, Carmillo P, Ehrenfels C, Picard JY, Cate
560 RL. Processing of anti-Müllerian hormone regulates receptor activation by a
561 mechanism distinct from TGF-β. Mol Endocrinol 2010;24:2193–206.
562 [36] Hirschhorn T, di Clemente N, Amsalem AR, Pepinsky RB, Picard JY, Smorodinsky
563 NI, Cate RL, Ehrlich M. Constitutive negative regulation in the processing of the
564 anti-Müllerian hormone receptor II. J Cell Sci 2015;128:1352-64.
565 [37] Rosas-Arellano A, Villalobos-González JB, Palma-Tirado L, Beltrán FA, Cárabez-
566 Trejo A, Missirlis F, Castro MA. A simple solution for antibody signal enhancement
567 in immunofluorescence and triple immunogold assays. Histochem Cell Biol
568 2016;146:421-30.
569 [38] Campbell RE, Gaidamaka G, Han SK, Herbison AE. Dendro-dendritic bundling and
570 shared synapses between gonadotropin-releasing hormone neurons. Proc Natl Acad
571 Sci U S A 2009;106:10835-40.
572 [39] Georgopoulos NA, Karagiannidou E, Koika V, Roupas ND, Armeni A, Marioli D,
573 Papadakis E, Welt CK, Panidis D. Increased frequency of the anti-mullerian-
574 inhibiting hormone receptor 2 (AMHR2) 482 A>G polymorphism in women with

575 polycystic ovary syndrome: relationship to luteinizing hormone levels. J Clin
576 Endocrinol Metab 2013;98:E1866-70.
577

578 **Table 1.** Details concerning the primers used for PCR to detect mRNA of anti-Müllerian

579 hormone (AMH) and anti-Müllerian hormone receptor type 2 (AMHR2).

580

Primer		5'-3'	Position		Product size (bp)
			Nucleotide	Exon	
AMH	up	GCTCATCCCCGAGACATACC	1486-1505	5	328
	down	TTCCCGTGTTTAATGGGGCA	1794-1813	5	
AMHR2	up	AGATTTGCGACCTGACAGCAG	1272-1292	9-10	320
	down	CTTCCAGGCAGCAAAGTGAG	1572-1591	11	

581

582 **Table 2.** Mean ± SEM of the number of examined GnRH-positive, AMHR2-positive, or
583 AMH-positive cell bodies (round or polygonal shape, diameter is more than 8 μm) and
584 fibers (axon shown as continuous line of immunopositive signal, or varicosity shown as
585 dotted line) in the preoptic area.
586

	POA cell body		**POA fiber**	
	Mean	SEM	Mean	SEM
GnRH+	27.0	0.5	31.0	0.5
AMHR2+	30.6	0.4	30.6	0.5
AMH+	30.0	1.1	31.6	0.8

587
588

589 **Table 3.**

590 (A) Mean ± SEM of the percentage of GnRH cells that co-localize AMHR2 or AMH, the

591 percentage of AMHR2 or AMH cells that co-localize GnRH in the POA.

592 (B)

	POA cell body	
	Mean	SEM
GnRH cells co-localize AMHR2	87.5	1.4
GnRH cells co-localize AMH	78.7	1.8
GnRH cells co-localize both AMHR2 and AMH	78.7	1.8
AMHR2 cells co-localize GnRH	77.1	0.3
AMH cells co-localize GnRH	70.9	1.9

593

594 (B) Mean ± SEM of the percentage of GnRH fibers that co-localize AMHR2 or AMH,

595 the percentage of AMHR2 or AMH fibers that co-localize GnRH in the POA.

596

	POA fibers	
	Mean	SEM
GnRH fibers co-localize AMHR2	82.8	3.0
GnRH fibers co-localize AMH	76.9	2.8
GnRH fibers co-localize both AMHR2 and AMH	76.9	2.8
AMHR2 fibers co-localize GnRH	83.6	0.3
AMH fibers co-localize GnRH	75.5	2.4

597

598 **Table 4.** Mean ± SEM of the number of examined GnRH-positive, AMHR2-positive, or
599 AMH-positive fibers in the arcuate nucleus (ARC) or internal (iME) or external zone of
600 median eminence (eME).

601

	ARC		iME		eME	
	Mean	SEM	Mean	SEM	Mean	SEM
GnRH+	21.6	0.7	22.8	0.4	56.4	0.9
AMHR2+	21.6	0.8	24.4	0.8	54.0	1.9
AMH+	20.2	0.7	22.4	1.2	53.4	1.4

602

603

604 **Table 5.** Mean ± SEM of the percentage of GnRH fibers that co-localize AMHR2 or AMH,
605 the percentage of AMHR2 or AMH fibers that co-localize GnRH in the ARC, iME, or
606 eME.
607

	ARC		iME		eME	
	Mean	SEM	Mean	SEM	Mean	SEM
GnRH fibers co-localize AMHR2	84.2	1.9	83.3	1.7	86.2	3.5
GnRH fibers co-localize AMH	76.7	1.8	74.6	0.8	84.7	3.3
GnRH fibers co-localize both AMHR2 and AMH	76.7	1.8	74.6	0.8	84.7	3.3
AMHR2 fibers co-localize GnRH	84.3	2.1	78.3	3.7	89.9	1.7
AMH fibers co-localize GnRH	82.1	2.1	76.6	3.5	89.4	2.4

608
609

Figure Legends

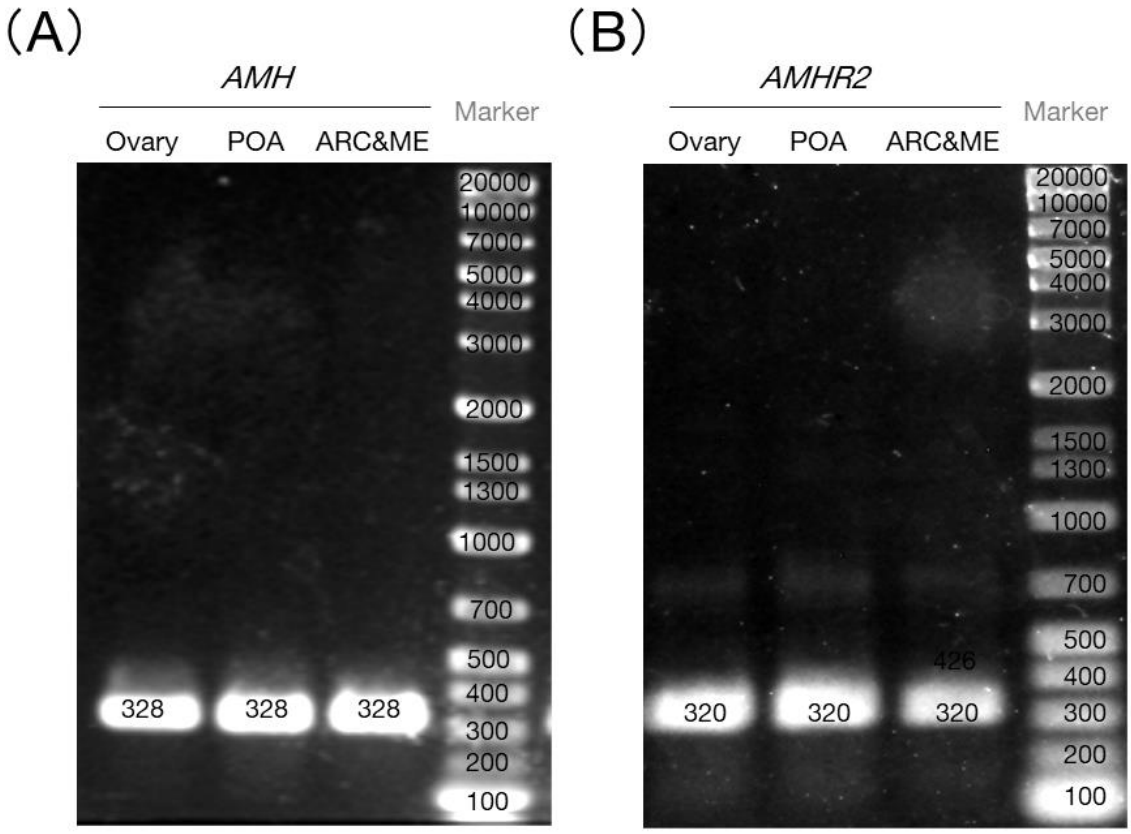

Fig. 1. Detection of anti-Müllerian hormone (AMH) mRNA (A) and AMH receptor type 2 (AMHR2) mRNA (B) by RT-PCR. Electrophoresis of PCR-amplified DNA products using primers for bovine AMH or AMHR2 and cDNA derived from the ovary, tissues containing the preoptic area (POA tissue), or arcuate nucleus and median eminence tissues (ARC&ME tissue) of post-pubertal heifers. The lanes labeled as AMH or AMHR2 demonstrate that the sizes of the obtained DNA products met expectations: 328 or 320 bp, respectively. The Marker lane indicates the DNA marker.

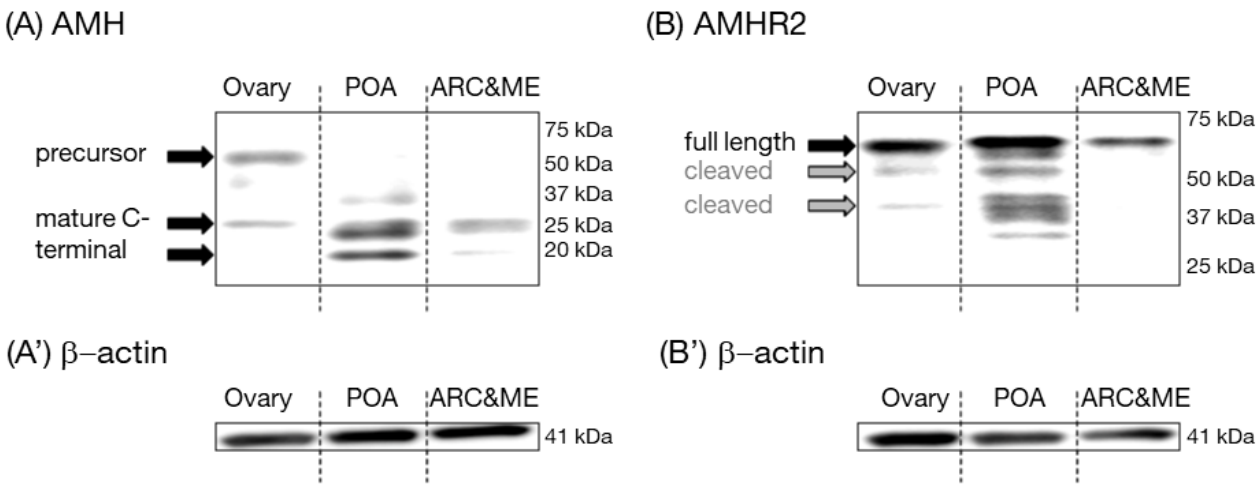

Fig. 2. Results of western blotting using extracts from the ovary, POA, or ARC&ME tissue of post-pubertal heifers and anti-AMH antibody (A), anti-AMHR2 antibody (B), or anti-β–actin antibody (A' and B'). Bovine AMH bands were defined based on size as either precursors or mature C-terminal proteins. Bovine AMHR2 bands were defined based on size as either full-length or cleaved monomers.

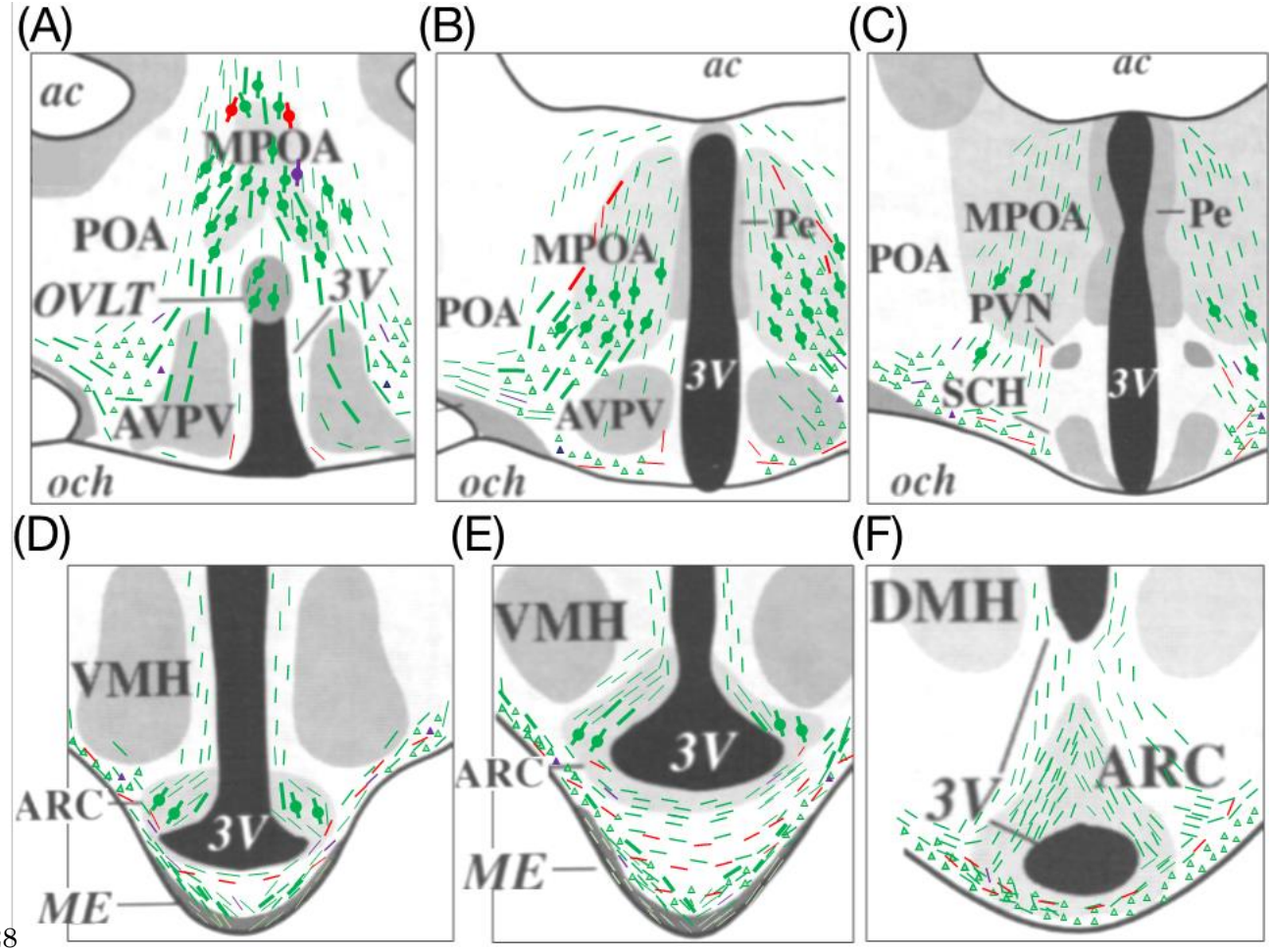

628

629 **Fig. 3.** Immunocytochemical distribution of GnRH, AMH and AMHR2 in coronal

630 sections containing POA (A, B, C), or ARC and ME (D, E, F) drawn on the corresponding

631 region of the bovine brain atlas [23]. The crosses, lines, and triangles indicate cell body,

632 and longitudinal and cross-section of fibers, respectively. The green ones indicate GnRH-

633 positive, AMH-positive and AMHR2-positive (triple positive). The red ones indicate

634 GnRH-positive AMH-negative and AMHR2-negative. The purple ones indicate lack of

635 colocalization of AMH and GnRH.

636 Abbreviations: 3V, third ventricle; ac, anterior commissure; och, optic chiasm; ARC,

arcuate nucleus; AVPV, anteroventral periventricular nucleus; DMH, dorsomedial hypothalamic nucleus; ME, median eminence; MPOA, medial preoptic area; OVLT, vascular organ of the lamina terminals; Pe, periventricular hypothalamic nucleus; PVN, paraventricular hypothalamic nucleus; POA, preoptic area; SCH, suprachiasmatic nucleus; VMH, ventromedial hypothalamic nucleus.

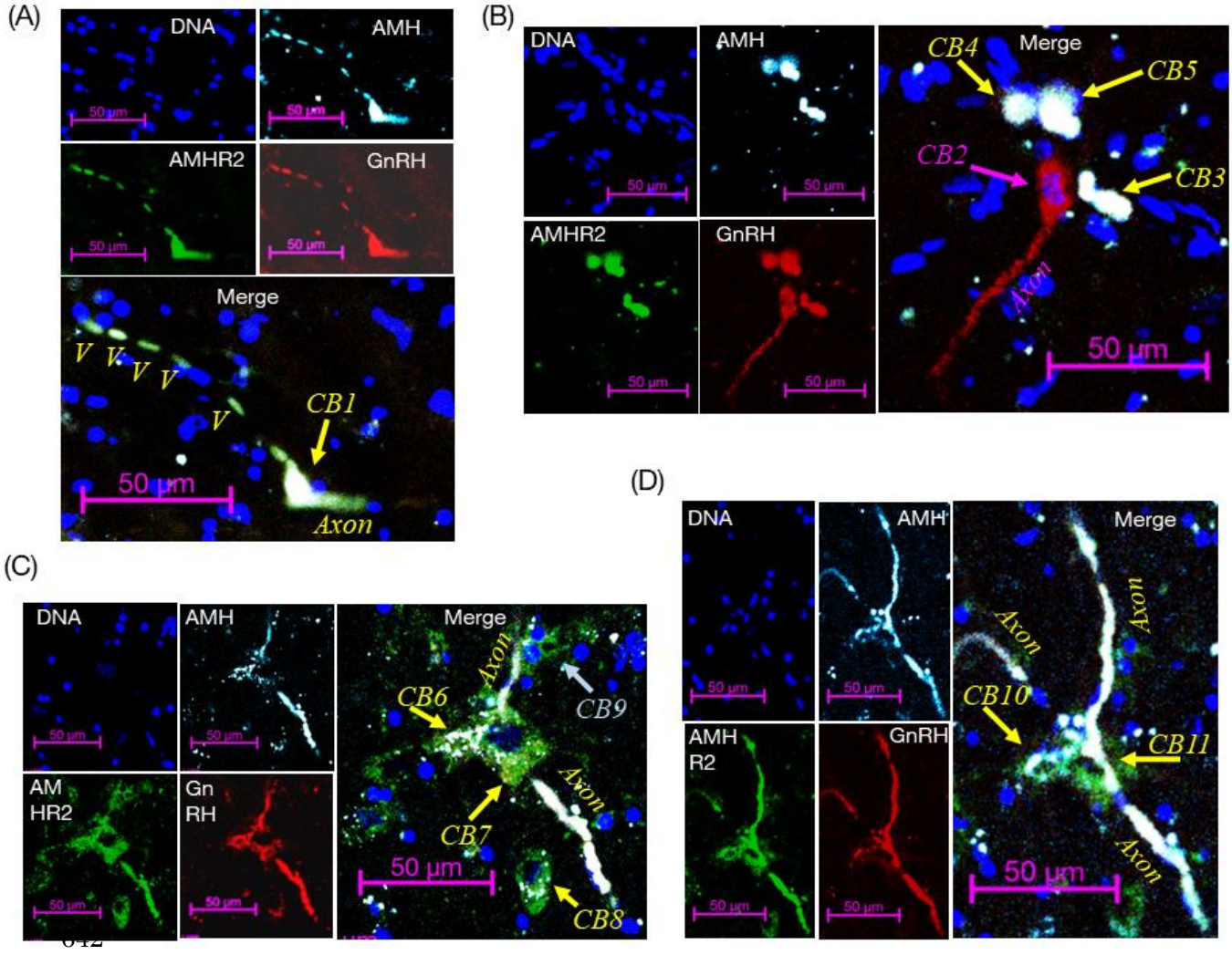

Fig. 4. Triple-fluorescence photomicrographs of AMH, AMHR2, and GnRH in the POA (A, B, C, D) of post-pubertal heifers. Images were captured with laser confocal microscopy for AMH (light blue), AMHR2 (green), and GnRH (red). In the merged photos, CB, Axon, V indicate cell body, axon, and varicosity of neuron. The yellow arrows, CB, Axon, and V indicate the colocalization of AMH, AMHR2, and GnRH. Light blue ones indicate lack of colocalization of AMH and GnRH. Red ones indicate lack of colocalization of GnRH and AMH or AMHR2. Scale bars are 50 μm.

(A)

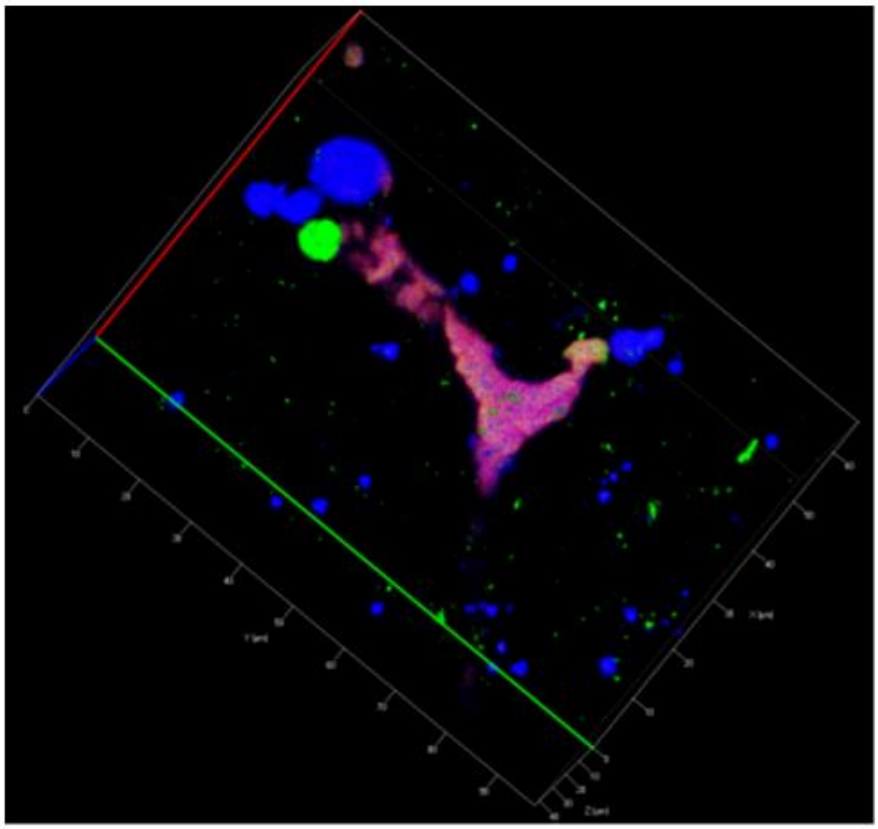

(B)

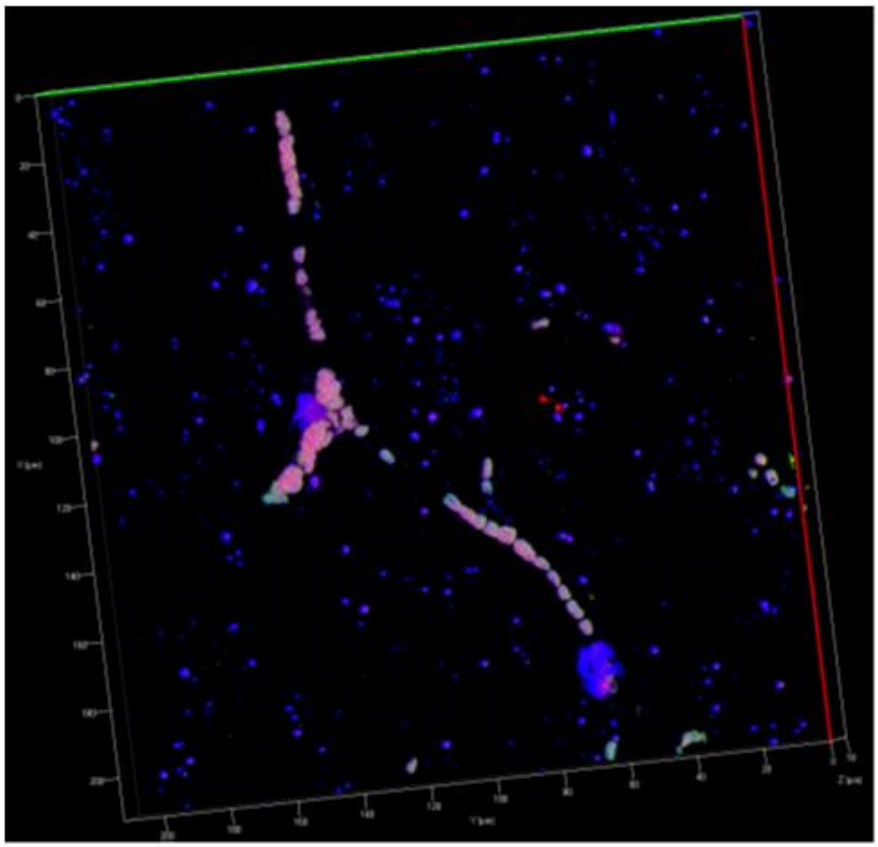

650

Fig. 5. Transparent projection of the z-stack images of triple-stained cell bodies and fibers in the POA (A, B) of post-pubertal heifers. The images were captured using a laser confocal microscope. AMH, AMHR2, and GnRH are depicted in blue, green, and red, respectively. Note that the color indicating DNA has been excluded because the large number of cell nuclei containing DNA would have masked the main objects.

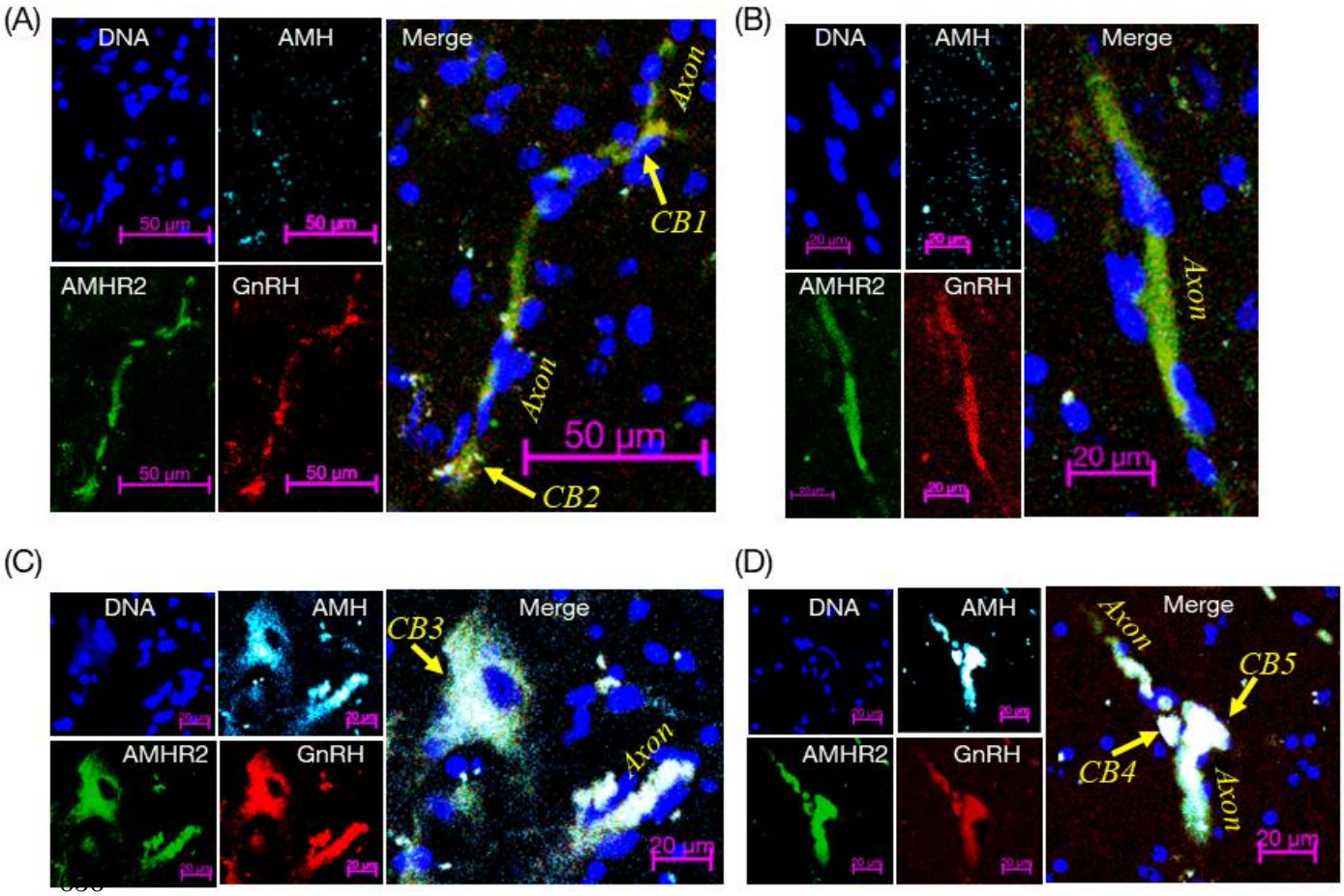

Fig. 6. Triple-fluorescence photomicrographs of ARC (A, B, C, D) tissue obtained from post-pubertal heifers. Images were captured with laser confocal microscopy for AMH (light blue), AMHR2 (green), and GnRH (red). In the merged photos, the yellow arrows CB, and Axon indicate the colocalization of AMH, AMHR2, and GnRH. Scale bars are 50 µm (A) or 20 µm (B, C, D).

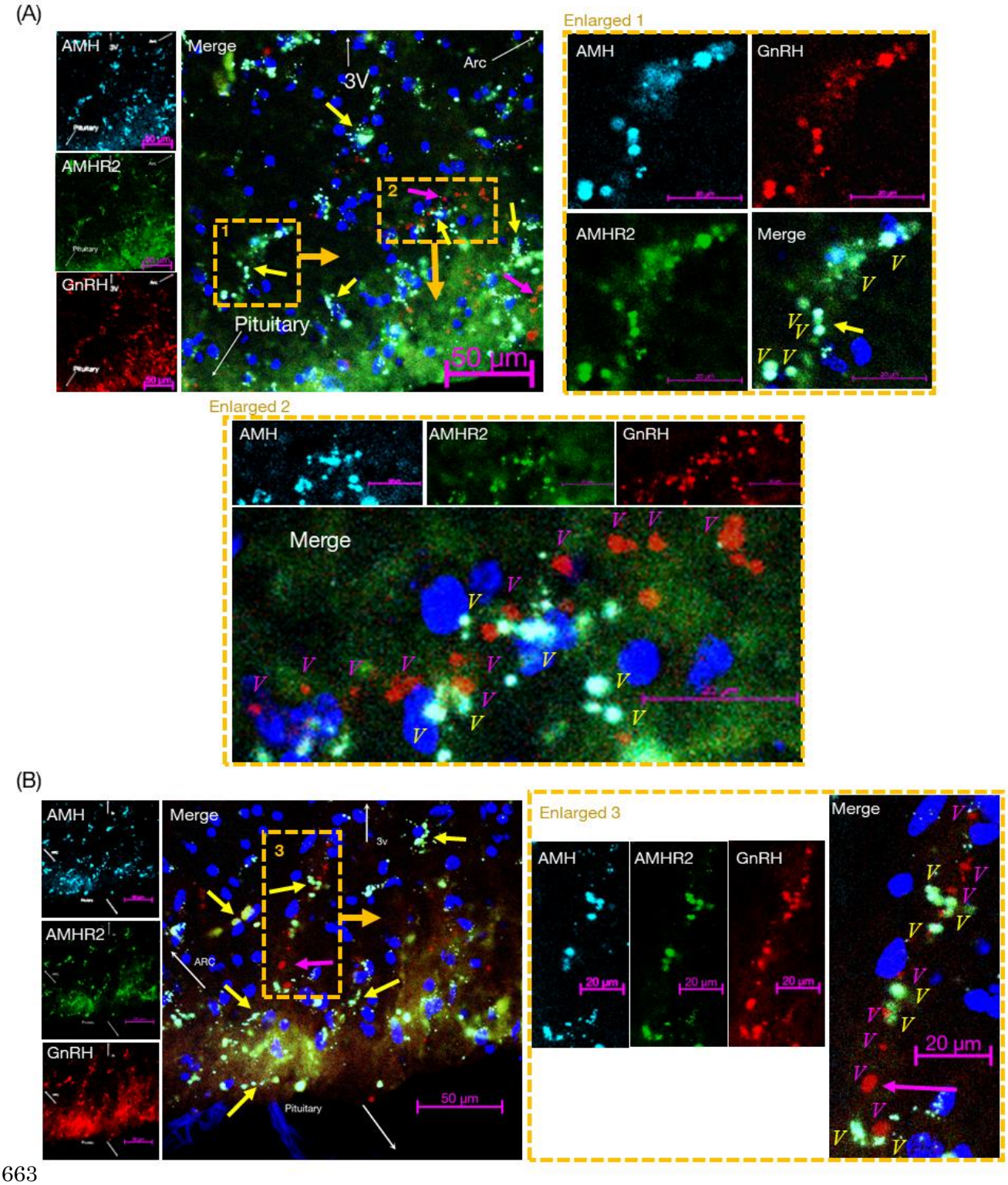
(A)
AMH
AMHR2
GnRH
Merge
3V
Arc
1
2
Pituitary
50 μm
Enlarged 1
AMH
GnRH
AMHR2
Merge
Enlarged 2
AMH
AMHR2
GnRH
Merge
(B)
AMH
AMHR2
GnRH
Merge
3
3v
ARC
Pituitary
50 μm
Enlarged 3
AMH
AMHR2
GnRH
20 μm
Merge
20 μm

663

664

665

Fig. 7. Triple-fluorescence photomicrographs of ME (A, B) tissue obtained from post-pubertal heifers. Images were captured with laser confocal microscopy for AMH (light blue), AMHR2 (green), and GnRH (red). The orange rectangle within the low magnification image indicates the position of high magnification. In the merged photos, the yellow arrows and V indicate the colocalization of AMH, AMHR2, and GnRH; the red arrows and V indicate the lack of colocalization of GnRH and AMH or AMHR2. Scale bars are 50 μm in the low-magnification photos of (A, B), and 20 μm in the high magnification photos of (A,B). White arrows labeled as 3V, Arc, or Pituitary indicate the direction of the third ventricle, arcuate nucleus, and pituitary, respectively.

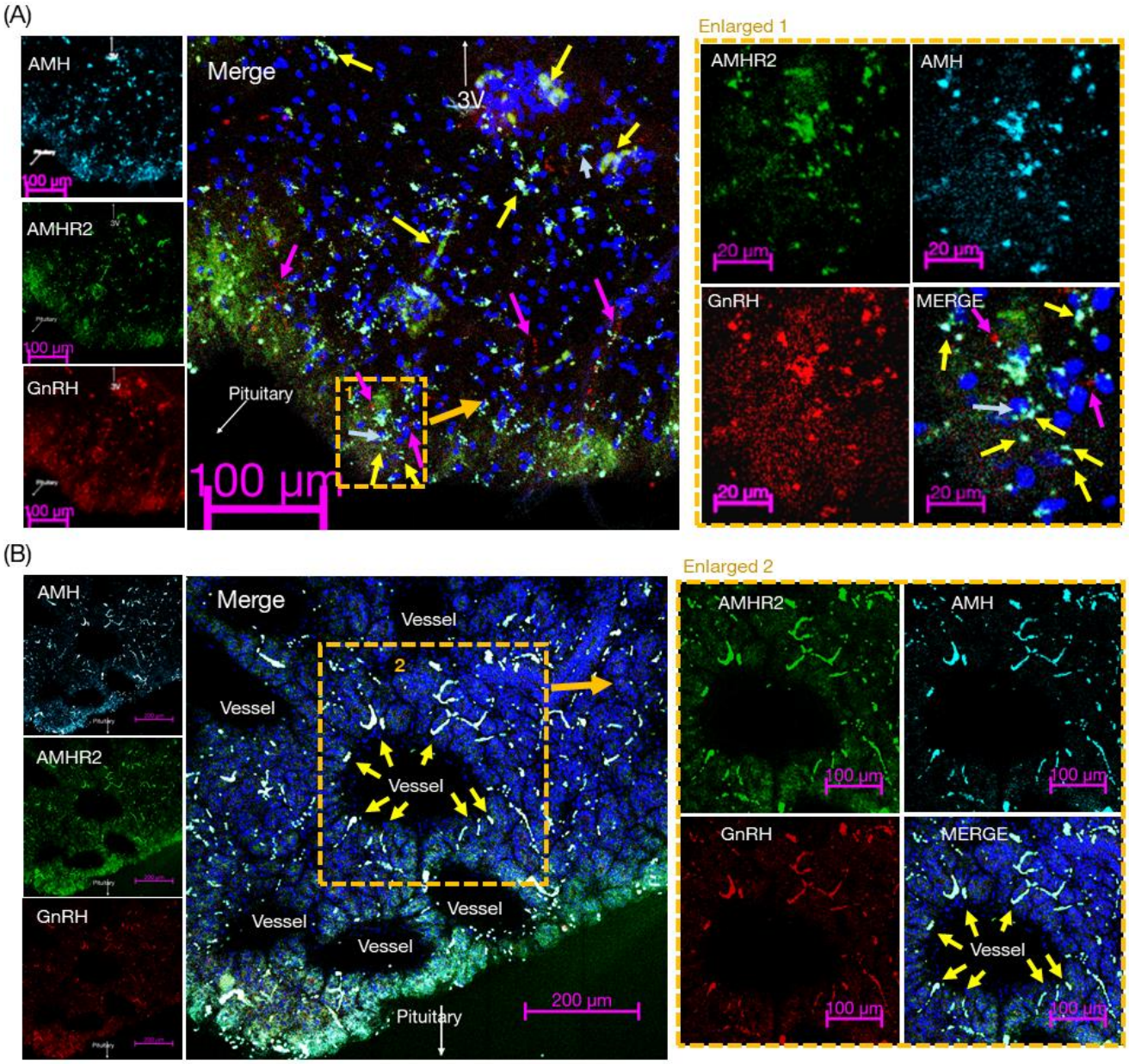

676

677 **Fig. 8.** Triple-fluorescence photomicrographs of other parts of ME (A, B) tissue obtained

678 from post-pubertal heifers. Images were captured with laser confocal microscopy for

679 AMH (light blue), AMHR2 (green), and GnRH (red). The orange rectangle within the

680 low magnification image indicates the position of high magnification. Vessel indicate the

681 position of vessel. In the merged photos, the yellow arrows indicate the colocalization of

682 AMH, AMHR2, and GnRH; the light blue arrows indicate the lack of colocalization of
683 AMH and GnRH; the red arrows and V indicate the lack of colocalization of GnRH and
684 AMH or AMHR2. Scale bars are 100 μm in the low-magnification photos of (A) and
685 high-magnification photos of (B), 20 μm in the high magnification photos of (A), and 200
686 μm in the low-magnification photos of (B). White arrows labeled as 3V, or Pituitary
687 indicate the direction of the third ventricle, and pituitary, respectively.
688

(A)

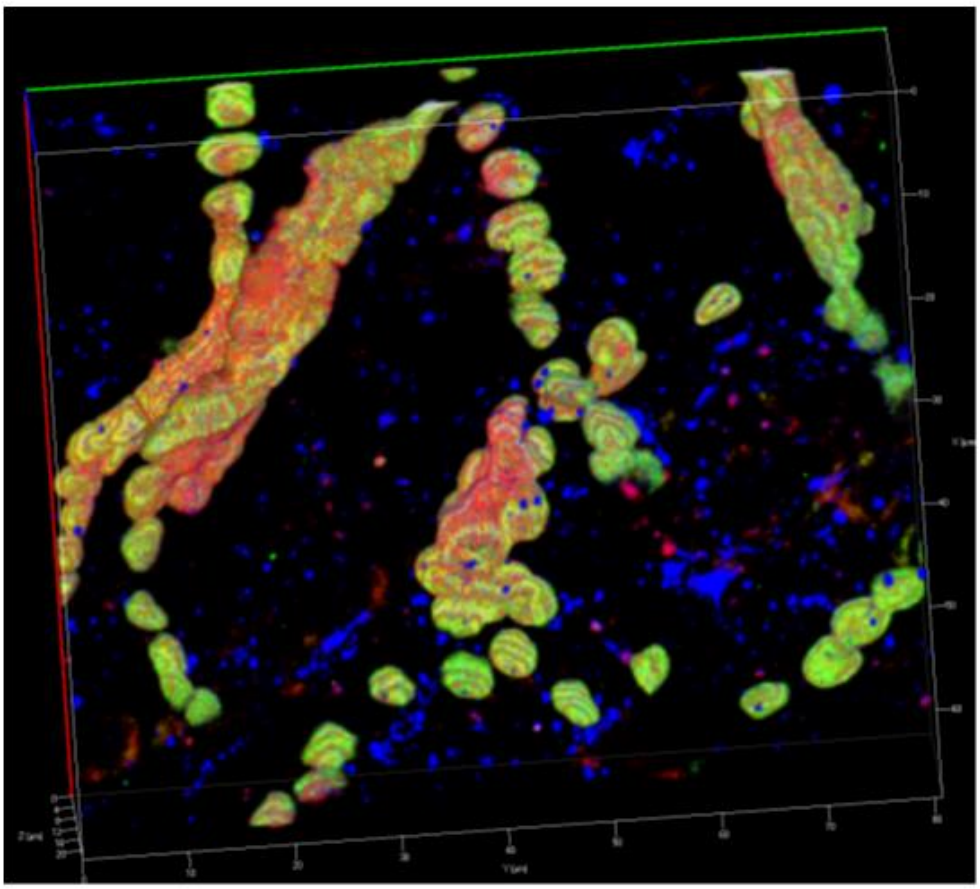

(B)

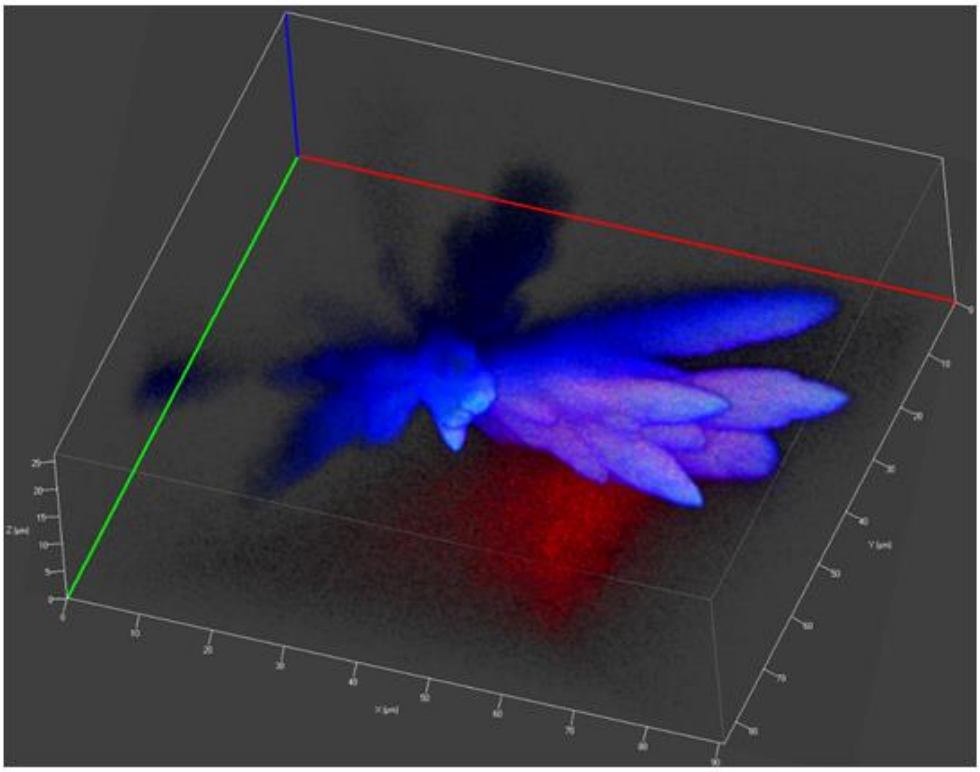

689

690 **Fig. 9.** Transparent projection of the z-stack images of triple-stained fibers (A) and
691 terminal (B) in the eME of post-pubertal heifers. The images were captured using a laser
692 confocal microscope. for AMH, AMHR2, and GnRH are depicted in blue, green, and red,
693 respectively. Note that the color indicative of DNA has been excluded because the large
694 number of cell nuclei containing DNA would have masked the main objects.